NASA/CR–2019-220403

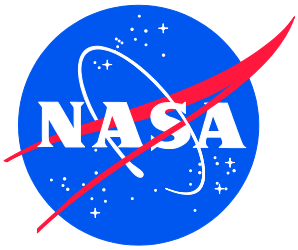

Design of a Slotted, Natural-Laminar-Flow Airfoil for a Transport Aircraft

Dan M. Somers
Airfoils Incorporated, Port Matilda, Pennsylvania

September 2019

NASA STI Program . . . in Profile

Since its founding, NASA has been dedicated to the advancement of aeronautics and space science. The NASA scientific and technical information (STI) program plays a key part in helping NASA maintain this important role.

The NASA STI program operates under the auspices of the Agency Chief Information Officer. It collects, organizes, provides for archiving, and disseminates NASA's STI. The NASA STI program provides access to the NTRS Registered and its public interface, the NASA Technical Reports Server, thus providing one of the largest collections of aeronautical and space science STI in the world. Results are published in both non-NASA channels and by NASA in the NASA STI Report Series, which includes the following report types:

- TECHNICAL PUBLICATION. Reports of completed research or a major significant phase of research that present the results of NASA Programs and include extensive data or theoretical analysis. Includes compilations of significant scientific and technical data and information deemed to be of continuing reference value. NASA counter-part of peer-reviewed formal professional papers but has less stringent limitations on manuscript length and extent of graphic presentations.

- TECHNICAL MEMORANDUM. Scientific and technical findings that are preliminary or of specialized interest, e.g., quick release reports, working papers, and bibliographies that contain minimal annotation. Does not contain extensive analysis.

- CONTRACTOR REPORT. Scientific and technical findings by NASA-sponsored contractors and grantees.

- CONFERENCE PUBLICATION. Collected papers from scientific and technical conferences, symposia, seminars, or other meetings sponsored or co-sponsored by NASA.

- SPECIAL PUBLICATION. Scientific, technical, or historical information from NASA programs, projects, and missions, often concerned with subjects having substantial public interest.

- TECHNICAL TRANSLATION. English-language translations of foreign scientific and technical material pertinent to NASA's mission.

Specialized services also include organizing and publishing research results, distributing specialized research announcements and feeds, providing information desk and personal search support, and enabling data exchange services.

For more information about the NASA STI program, see the following:

- Access the NASA STI program home page at *http://www.sti.nasa.gov*

- E-mail your question to help@sti.nasa.gov

- Phone the NASA STI Information Desk at 757-864-9658

- Write to:

NASA STI Information Desk
Mail Stop 148
NASA Langley Research Center
Hampton, VA 23681-2199

NASA/CR–2019-220403

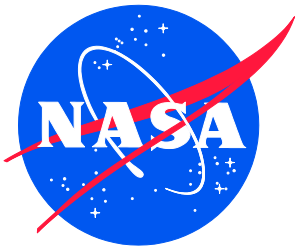

Design of a Slotted, Natural-Laminar-Flow Airfoil for a Transport Aircraft

Dan M. Somers
Airfoils Incorporated, Port Matilda, Pennsylvania

National Aeronautics and
Space Administration

Langley Research Center
Hampton, Virginia 23681-2199

Prepared for Langley Research Center
under Contract NNX17AJ95A

September 2019

Available from:

NASA STI Program / Mail Stop 148
NASA Langley Research Center
Hampton, VA 23681-2199
Fax: 757-864-6500

DESIGN OF A SLOTTED, NATURAL-LAMINAR-FLOW AIRFOIL FOR A TRANSPORT AIRCRAFT

DAN M. SOMERS

AUGUST 2019

AIRFOILS, INCORPORATED

PORT MATILDA, PENNSYLVANIA

DESIGN OF A SLOTTED, NATURAL-LAMINAR-FLOW AIRFOIL FOR A TRANSPORT AIRCRAFT

DAN M. SOMERS

AUGUST 2019

ABSTRACT

A 13.49-percent-thick, slotted, natural-laminar-flow airfoil, the S207, for a transport aircraft has been designed and analyzed theoretically. The two primary objectives of high maximum lift, insensitive to roughness, and low profile drag have been achieved. The drag-divergence Mach number is predicted to be greater than 0.70.

INTRODUCTION

The wing profile drag is the largest contributor to the total aircraft drag at cruise conditions for most aircraft because of the generally low lift coefficients and correspondingly low induced drag. The wing profile drag contributes about one third of the total drag for transport aircraft. As the aircraft size decreases from transport through regional to business jets and other general-aviation (GA) aircraft and finally unmanned aerial vehicles (UAVs) and sailplanes, the percentage of the total aircraft drag due to the wing profile drag generally increases, as shown in the following table, primarily because the relative wing area increases and the chord Reynolds number decreases.

Aircraft Type	$\frac{\text{Wing Profile Drag}}{\text{Total Aircraft Drag}}$
Transport	~ 1/3
Business jet	~ 1/3
Low-speed general aviation	> 1/3
Unmanned aerial vehicle	1/3 to 1/2
Sailplane	> 1/2

To minimize wing profile drag, the figure of merit FOM applicable to aircraft having their wing area determined by a minimum-speed requirement (usually landing speed) should be maximized:

$$\text{FOM} = \frac{c_{l,\,\max}}{c_{\text{d, cruise}}}$$

where $c_{l,\max}$ is the section maximum lift coefficient and $c_{d,\text{cruise}}$ is the cruise section profile-drag coefficient. (See Ref. 1.) Note that the figure of merit is expressed in terms of section (airfoil) characteristics, not aircraft characteristics. The figure of merit can be interpreted as follows. The wing area, and therefore the aircraft wetted area, can be reduced if a higher maximum lift coefficient is achieved, resulting in lower drag. The wing profile drag can also be reduced if a lower section profile-drag coefficient is achieved. This figure of merit applies to almost all aircraft types. For those aircraft having their wing area determined by a fuel-volume requirement (e.g., business jets), reducing the section profile-drag coefficient is even more beneficial.

Three approaches have become accepted for the reduction of wing profile drag. One approach is to employ a high-lift system (e.g., leading-edge slat plus double- or triple-slotted, Fowler flap) to achieve a higher maximum lift coefficient (see Ref. 2, for example). This approach has several disadvantages. Almost no laminar flow can be achieved because of the disturbances introduced by the slat, which results in a high section profile-drag coefficient. The maximum lift coefficient is limited to about 4, which limits the reduction in wing area. High-lift systems are complex, both mechanically and structurally, resulting in higher weight and cost. This approach can provide a maximum wing profile-drag reduction of about 50 percent compared to a conventional, turbulent-flow wing with no high-lift system and has been adopted for all current transport aircraft. Active high-lift systems (e.g., blown flaps and circulation control) have demonstrated very high lift coefficients, but the cost, complexity, and potentially disastrous failure modes have prevented their adoption in production aircraft.

A second approach is to employ a natural-laminar-flow (NLF) airfoil to achieve a lower profile-drag coefficient (see Ref. 3, for example). By appropriate airfoil shaping, extensive ($\geq$ 30-percent-chord) laminar flow can be achieved on both the upper and lower wing surfaces. The extent of laminar flow is limited to about 70-percent chord by the pressure-recovery gradient along the aft portion of the airfoil and by leading-edge sweep. The recovery gradient becomes steeper as the extent of the favorable gradient along the forward portion of the airfoil increases, eventually reaching a limit beyond which trailing-edge separation occurs, resulting in a lower maximum lift coefficient and, correspondingly, a lower figure of merit. Leading-edge sweep restricts the extent of laminar flow because it introduces crossflow instabilities that lead to transition. This approach can also provide a wing profile-drag reduction of about 50 percent compared to a conventional, turbulent-flow wing and has been adopted for most current general-aviation aircraft, including business jets, as well as unmanned aerial vehicles and all sailplanes. It does, however, require more stringent construction techniques.

A third approach is to employ a laminar-flow-control (LFC) airfoil to achieve a lower profile-drag coefficient (see Ref. 4, for example). By incorporating suction through porous or slotted, wing skins, 100-percent-chord laminar flow can be achieved on both the upper and lower wing surfaces. LFC systems are very complex, mechanically, structurally, and operationally, resulting in higher weight and cost. This approach can provide a wing profile-drag reduction of about 75 percent compared to a conventional, turbulent-flow wing but has yet to be adopted for any production aircraft.

For the present effort, a new approach, called a slotted, natural-laminar-flow (SNLF) airfoil (Ref. 5), is employed. The SNLF airfoil concept is similar in nature to the slotted, supercritical airfoil concept (Ref. 6), in that it employs a slot to allow a pressure recovery that would not be possible for a single-element airfoil.

SYMBOLS

C_p	pressure coefficient
c	airfoil chord, m
c_d	section profile-drag coefficient
c_l	section lift coefficient
c_m	section pitching-moment coefficient about quarter-chord point
M	free-stream Mach number
Re	Reynolds number based on free-stream conditions and airfoil chord
t	airfoil thickness, m
x	airfoil abscissa, m
α	angle of attack relative to x-axis, deg

Subscripts:

ll	lower limit of low-drag range
ls	lower surface
max	maximum
T	transition
ul	upper limit of low-drag range
us	upper surface
0	zero lift

Abbreviations:

LFC	laminar flow control
NASA	National Aeronautics and Space Administration
NLF	natural laminar flow

SNLF slotted, natural laminar flow

ULI NASA University Leadership Initiative

AIRFOIL DESIGN

OBJECTIVES AND CONSTRAINTS

The design specifications for the airfoil are contained in Table I. The specifications were initially developed from the Boeing Subsonic Ultra Green Aircraft Research (SUGAR) aircraft (Ref. 7) and later refined in cooperation with other members of our University Leadership Initiative Configuration Technical Sub-Group, especially the Pennsylvania State University and University of Tennessee researchers.

Two primary objectives are evident. The first objective is to achieve a maximum lift coefficient of 2.30 at a Mach number of 0.225 and a Reynolds number of 16.0×10^6, based on the mean aerodynamic wing chord at minimum speed. A requirement related to this objective is that the maximum lift coefficient not decrease significantly with transition fixed near the leading edge on all surfaces. In addition, the airfoil should exhibit docile stall characteristics. The second objective is to obtain low profile-drag coefficients over the range of lift coefficients from 0.39 to 0.65 at a Mach number of at least 0.660 and a Reynolds number of 13.2×10^6, based on the mean aerodynamic wing chord at the cruise condition.

No major constraints (e.g., zero-lift pitching-moment coefficient or airfoil thickness) were placed on the design of the airfoil.

PHILOSOPHY

Given the above objectives and constraint, certain characteristics of the design are apparent. The following sketch illustrates a drag polar that meets the goals for this design.

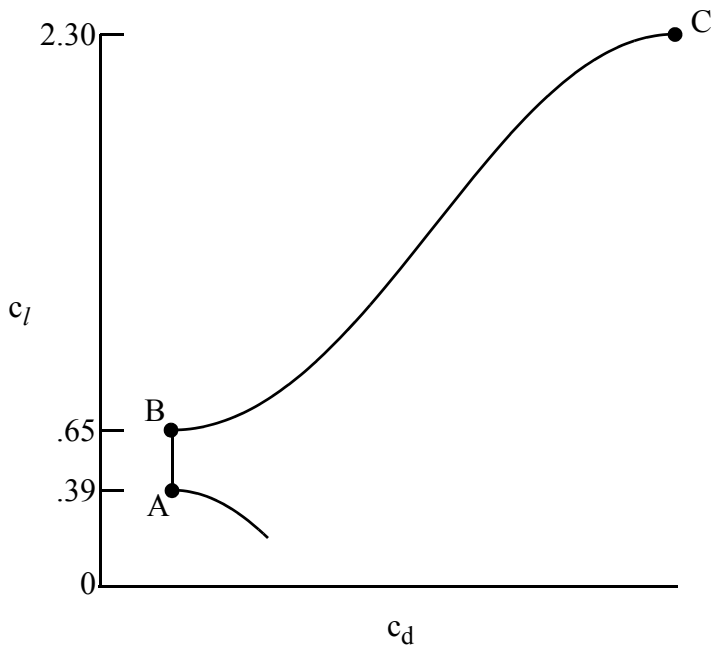

Sketch 1.- Drag polar that meets design goals.

Point A is the lower limit of the low-drag, lift-coefficient range; point B, the upper limit. The profile-drag coefficient increases very rapidly outside the low-drag range because boundary-layer transition moves quickly toward the leading edge with increasing (or decreasing) lift coefficient. This feature results in a leading edge that produces a suction peak at higher lift coefficients, which ensures that transition on the upper surface will occur very near the leading edge. Thus, the maximum lift coefficient, point C, occurs with turbulent flow along the entire upper surface and, therefore, should be relatively insensitive to roughness at the leading edge.

A two-element airfoil concept is used to meet the design requirements. The pressure distribution at point B is illustrated in sketch 2.

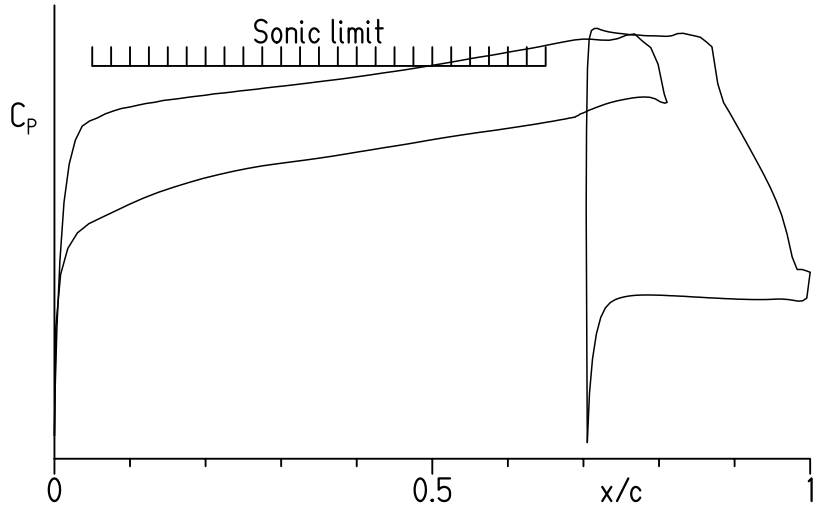

Sketch 2.- Pressure distribution for two-element airfoil concept.

Because the aft element eliminates the requirement that the pressure at the trailing edge of the fore element recover to free stream (see Ref. 8), the favorable pressure gradient can extend farther aft. For the slotted, natural-laminar-flow (SNLF) airfoil concept, the favorable gradient extends along both surfaces of the fore element to near its trailing edge. Thus, the fore element is essentially entirely laminar. The aft element then provides the necessary recovery to free-stream pressure. Because the wake of the fore element does not impinge on the aft element and because of its lower Reynolds number, the aft element can also achieve significant extents of laminar flow, even without favorable pressure gradients.

The SNLF airfoil concept allows the extent of natural laminar flow to be increased beyond the limit for NLF airfoils previously discussed. Thus, the concept allows lower section profile-drag coefficients to be achieved without having to resort to the complexity and cost of laminar flow control. The concept also achieves a high maximum lift coefficients without variable geometry (i.e., the aft element need not be deflected). The SNLF airfoil shape is not radically different from conventional airfoil shapes—no more than conventional, NLF airfoil shapes are from conventional, turbulent-flow airfoils. Unlike conventional airfoils with slotted flaps, however, the SNLF airfoil has no nested configuration; the slot between the fore and aft elements is always open.

EXECUTION

The Eppler Airfoil Design and Analysis Code (Refs. 9 and 10), a subcritical, single-element code, was used to design the initial fore- and aft-element shapes. The MSES code (Ref. 11), a transonic, multielement code, was used to refine the shapes in the two-element configuration. The resulting shapes contained four irregularities in the surface curvature that were alleviated mathematically by James G. Coder of the University of Tennessee.

The airfoil is designated the S207; its shape is shown in figure 1. The airfoil coordinates are available from Airfoils, Incorporated. The airfoil thickness is 13.49-percent chord.

THEORETICAL PROCEDURE

The theoretical results are predicted using the method of reference 11. A critical amplification factor of 9 was specified for the computations. Because of a laminar separation bubble predicted near the trailing edge of the fore element, however, transition was fixed on the upper surface of the fore element at 98 percent of the fore-element chord (i.e., $x/c \approx 0.79$). At a Mach number of 0.700 and a Reynolds number of 13.2×10^6, the method of reference 11 failed to converge for any angle of attack just beyond the upper limit of the low-drag, lift-coefficient range, preventing the definition of that portion of the drag polar. Note also that the method of reference 11 does not model the effect of Görtler instabilities (Ref. 12) on the laminar boundary layer. A cursory evaluation of this effect indicates that these instabilities may lead to transition in the concave region of the lower surface of the fore element.

Computations were also performed with transition fixed at 2-percent chord on the upper surface and 5-percent chord on the lower surface of both elements for a Mach number of 0.700 and a Reynolds number of 13.2×10^6. To account for the more aft location of the stagnation point at high lift coefficients, transition was fixed at the same locations on the aft element and on the upper surface of the fore element but at 10-percent chord on the lower surface of the fore element for a Mach number 0.225 and a Reynolds number of 16.0×10^6. Note that all the fixed-transition locations are specified relative to the chord of the respective element.

Because the right sides of the figures showing the transition locations and section characteristics contain several curves, an explanatory example with transition free is given in sketch 3, where the various curves are plotted with different line types. Note that the transition locations on the aft element are downstream of those on the fore element.

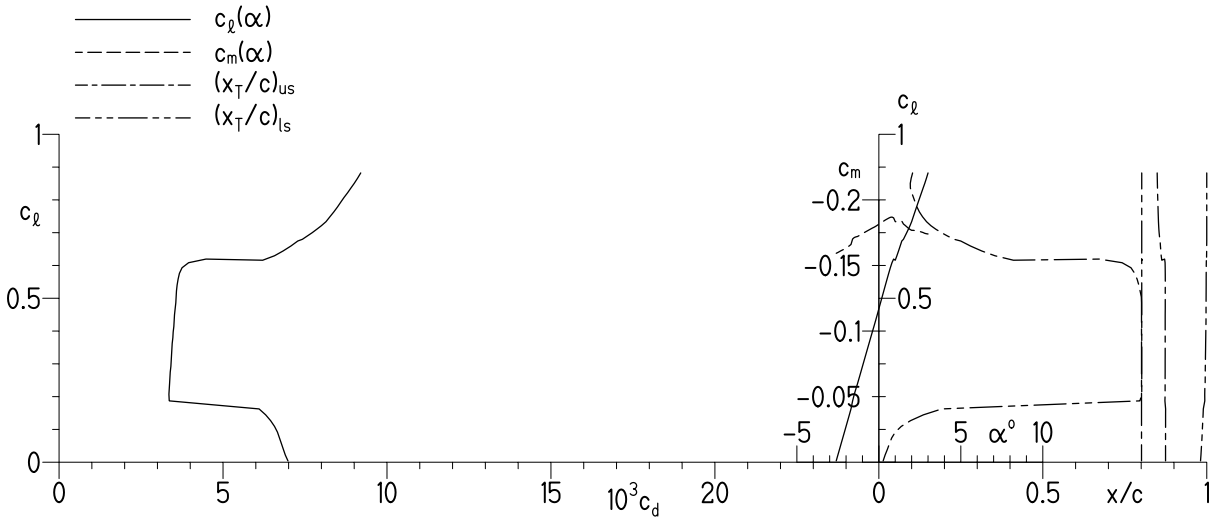

Sketch 3.- Explanatory example for transition-free figures.

DISCUSSION OF RESULTS

Traditionally, aerodynamic results are presented in order of increasing Mach number. Because the higher priority, cruise condition drives so much of this design, however, the higher Mach number results are presented first.

PRESSURE DISTRIBUTIONS

The pressure distributions at various angles of attack with transition free at a Mach number of 0.700 and a Reynolds number of 13.2×10^6 are shown in figure 2. At an angle of attack of –2.6° (Fig. 2(a)), which is just below the lower limit of the low-drag, lift-coefficient range, the pressure gradient along the upper surface of the fore element is favorable almost to the trailing edge, whereas the gradient along the lower surface of the fore element becomes steeply adverse around the entrance to the slot. At an angle of attack of –2.5° (Fig. 2(a)), which is within the low-drag range, the pressure gradient remains favorable along the entire lower surface of the fore element. At an angle of attack of –0.7° (Fig. 2(b)), which is just below the upper limit of the low-drag range, the pressure gradients along both surfaces of the fore element are favorable almost to the trailing edge. At an angle of attack of –0.6° (Fig. 2(b)), which is just above the upper limit of the low-drag range, the pressure gradient

along the upper surface of the fore element just forward of the trailing edge is slightly adverse, indicating that transition has moved forward to that location. Within the low-drag range, the pressure distribution on the aft element varies little with angle of attack.

The pressure distributions at various angles of attack with transition free at a Mach number of 0.225 and a Reynolds number of 16.0×10^6 are shown in figure 3. As the angle of attack is increased, a pressure peak forms at the leading edge of the fore element. The flow along the upper surface of the fore element has become supersonic at an angle of attack of 14.0° (Fig. 3(b)). Again, the pressure distribution on the aft element is relatively unaffected by angle of attack.

The effect of Mach number on the pressure distribution at an angle of attack of –1.3° for the cruise Reynolds number with transition free is shown in figure 4. This angle of attack is just below the upper limit of the low-drag range for the lower Mach number and well within the range for the higher Mach number. The pressure gradient, particularly along the upper surface of the fore element, becomes less favorable with decreasing Mach number, which is a typical, compressibility effect. The comparison also illustrates the sensitivity to Mach number of the pressure distribution along the lower surface of the fore element near the slot entrance. The pressure gradient forward of the pressure recovery on the upper surface of the aft element is affected as well.

TRANSITION LOCATION

The variations of boundary-layer transition location on the fore and aft elements with lift coefficient at a Mach number of 0.700 and a Reynolds number of 13.2×10^6 are shown in figure 5. Within the low-drag range, laminar flow extends essentially to the trailing edge on both surfaces of the fore element, to about 55 percent of the aft-element chord on its upper surface, and to the trailing edge on the lower surface of the aft element.

The variations of transition location on the fore and aft elements with lift coefficient at a Mach number of 0.225 and a Reynolds number of 16.0×10^6 are shown in figure 6. Transition on the upper surface of the fore element moves to the leading edge as the lift coefficient approaches maximum, which is a design feature, as previously discussed.

SECTION CHARACTERISTICS

The section characteristics at a Mach number of 0.700 and a Reynolds number of 13.2×10^6 with transition free are shown in figure 5. Low profile-drag coefficients are predicted over the range of lift coefficients from 0.37 to 0.74. Thus, the lower limit of the low-drag range is lower than the design objective of 0.39, and the upper limit is higher than the design objective of 0.65. Within the low-drag range, essentially no wave drag is predicted. The pitching-moment coefficient at a lift coefficient of 0.65 is –0.226. The drag-divergence Mach number with transition free is predicted to be greater than 0.70.

The section characteristics at a Mach number of 0.225 and a Reynolds number of 16.0×10^6 with transition free are shown in figure 6. The maximum lift coefficient is predicted to be 2.13, which is lower than the design objective of 2.30. Based on the predictions from the method of reference 11, the maximum lift coefficient appears to be limited by supersonic flow near the leading edge of the fore element (see Fig. 3(b)), making it difficult to assess the stall characteristics.

Effect of Mach Number

The effect of Mach number on the section characteristics for the cruise Reynolds number with transition free is shown in figure 7. The width of the low-drag range decreases significantly as the Mach number decreases from 0.700 to 0.650 because the pressure gradient, particularly along the upper surface of the fore element, becomes less favorable with decreasing Mach number, leading to earlier transition. (See Fig. 4.) The lift-curve slope and the magnitude of the pitching-moment coefficients decrease with decreasing Mach number, which are typical results.

The effect of Mach number on the section characteristics for the minimum-speed Reynolds number with transition free is shown in figure 8. The maximum lift coefficient increases as the Mach number decreases from 0.225 to 0.200, primarily because the supersonic flow on the upper surface of the fore element is delayed to higher angles of attack.

Effect of Fixing Transition

The effect of fixing transition on the section characteristics for the cruise condition is shown in figure 9. The lift-curve slope and the magnitude of the pitching-moment coefficients decrease with transition fixed. These results are principally a consequence of the boundary-layer displacement effect, which decambers the airfoil because the displacement thickness is greater with transition fixed than with transition free. The drag coefficients are, of course, adversely affected. The drag increase is larger than that for a single-element airfoil of the same thickness, however, because of the greater wetted surface length of a two-element configuration.

The effect of fixing transition on the section characteristics for the minimum-speed condition is shown in figure 10. The maximum lift coefficient with transition fixed is predicted to be 2.11, a decrease of less than 1 percent from that with transition free, which satisfies the design requirement.

If Görtler instabilities (Ref. 12) were to cause transition where the curvature of the lower surface of the fore element becomes concave, the drag coefficient for the cruise condition would increase by about 25 percent (Fig. 11), although the drag would still be low. All the other section characteristics would be unaffected.

CONCLUDING REMARKS

A 13.49-percent-thick, slotted, natural-laminar-flow airfoil, the S207, for a transport aircraft has been designed and analyzed theoretically. The two primary objectives of a high maximum lift coefficient, insensitive to leading-edge roughness, and low profile-drag coefficients have been achieved. The drag-divergence Mach number is predicted to be greater than 0.70.

ACKNOWLEDGMENTS

This effort was sponsored by the University of Tennessee as part of their Cooperative Agreement with the National Aeronautics and Space Administration (NASA) under the University Leadership Initiative (ULI).

REFERENCES

1. Maughmer, Mark D.; and Somers, Dan M.: Figures of Merit for Airfoil/Aircraft Design Integration. AIAA Paper 88-4416, Sept. 1988.

2. Smith, A. M. O.: High-Lift Aerodynamics. AIAA Paper 74-939, Aug. 1974.

3. Jacobs, Eastman N.: Preliminary Report on Laminar-Flow Airfoils and New Methods Adopted for Airfoil and Boundary-Layer Investigations. NACA WR L-345, 1939 (formerly, NACA ACR).

4. Pfenninger, Werner: Investigations on Reductions of Friction on Wings, in Particular by Means of Boundary Layer Suction. NACA TM 1181, 1947. (Translated from Mitteilungen aus dem Institut für Aerodynamik an der Eidgenössischen Technischen Hochschule Zürich, Nr. 13, 1946.)

5. Somers, Dan M.: Laminar-Flow Airfoil. U.S. Patent 6,905,092 B2, June 2005.

6. Whitcomb, Richard T.; and Clark, Larry R.: An Airfoil Shape for Efficient Flight at Supercritical Mach Numbers. NASA TM X-1109, 1965.

7. Bradley, Marty K.; and Droney, Christopher K.: Subsonic Ultra Green Aircraft Research Phase II: N+4 Advanced Concept Development. NASA/CR–2012-217556, 2012.

8. Maughmer, Mark D.: Trailing Edge Flow Conditions as a Factor in Airfoil Design. Ph.D. Dissertation, Univ. of Illinois, 1983.

9. Eppler, Richard: Airfoil Design and Data. Springer-Verlag (Berlin), 1990.

10. Eppler, Richard: Airfoil Program System "PROFIL11." User's Guide. Richard Eppler, c.2011.

11. Drela, M.: Design and Optimization Method for Multi-Element Airfoils. AIAA Paper 93-0969, Feb. 1993.

12. Görtler, H.: On the Three-Dimensional Instability of Laminar Boundary Layers on Concave Walls. NACA TM 1375, 1954.

Table I.- Airfoil Design Specifications.

Parameter	Value	Mach Number M	Reynolds Number Re	Priority
Maximum lift coefficient $c_{l,max}$	2.30	0.225	16.0×10^6	2
Lower limit of low-drag, lift-coefficient range $c_{l,ll}$	0.39	≥ 0.660	13.2×10^6	3
Upper limit of low-drag, lift-coefficient range $c_{l,ul}$	0.65			1
Zero-lift pitching-moment coefficient $c_{m,0}$	—			
Thickness t/c	—			

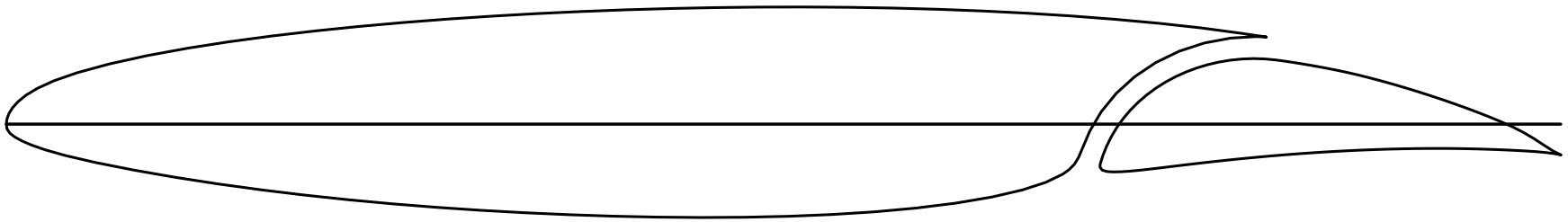

Figure 1.- S207 airfoil shape.

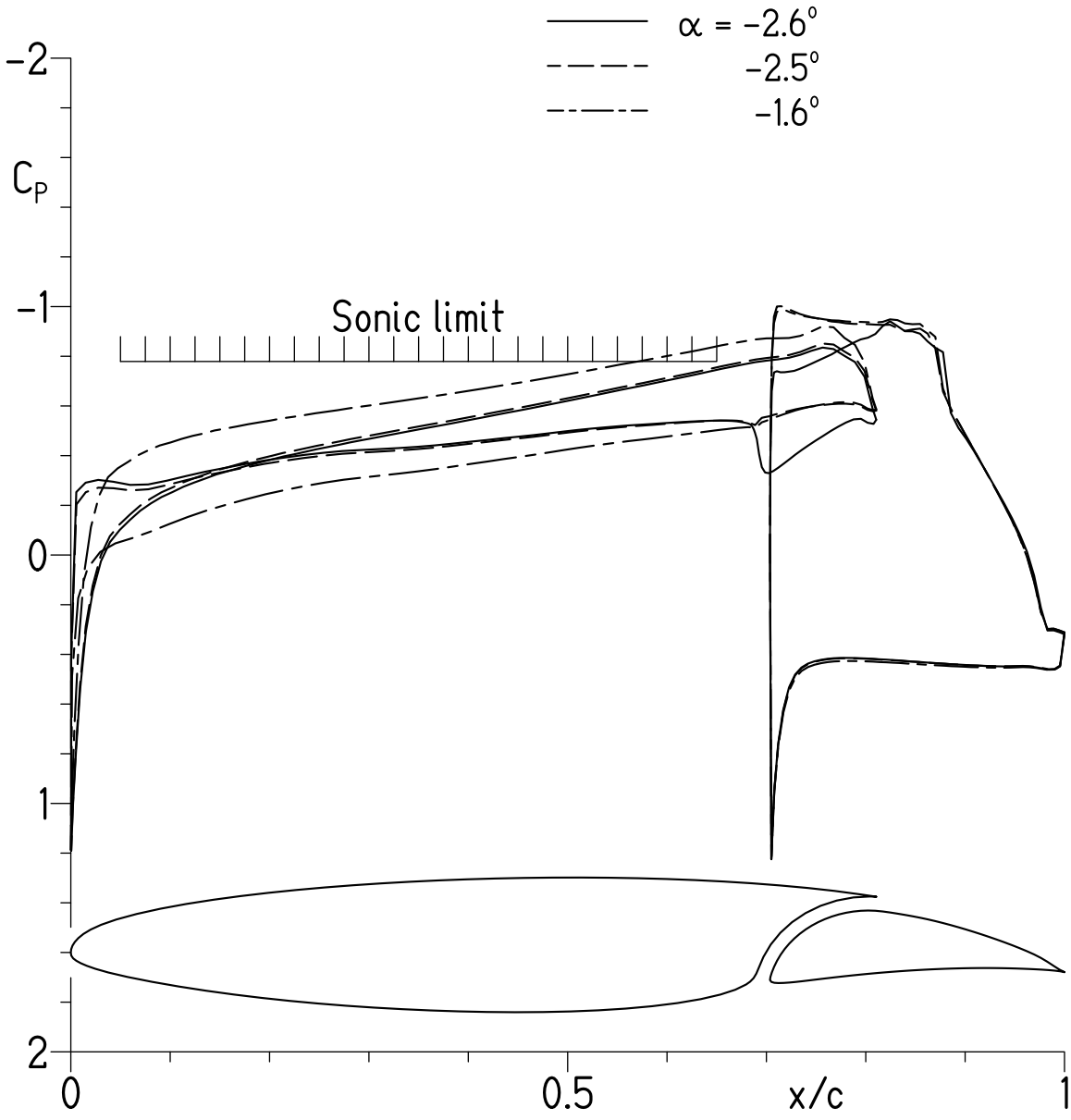

(a) $\alpha = -2.6°, -2.5°$, and $-1.6°$.

Figure 2.- Pressure distributions at $M = 0.700$ and $Re = 13.2 \times 10^6$ with transition free.

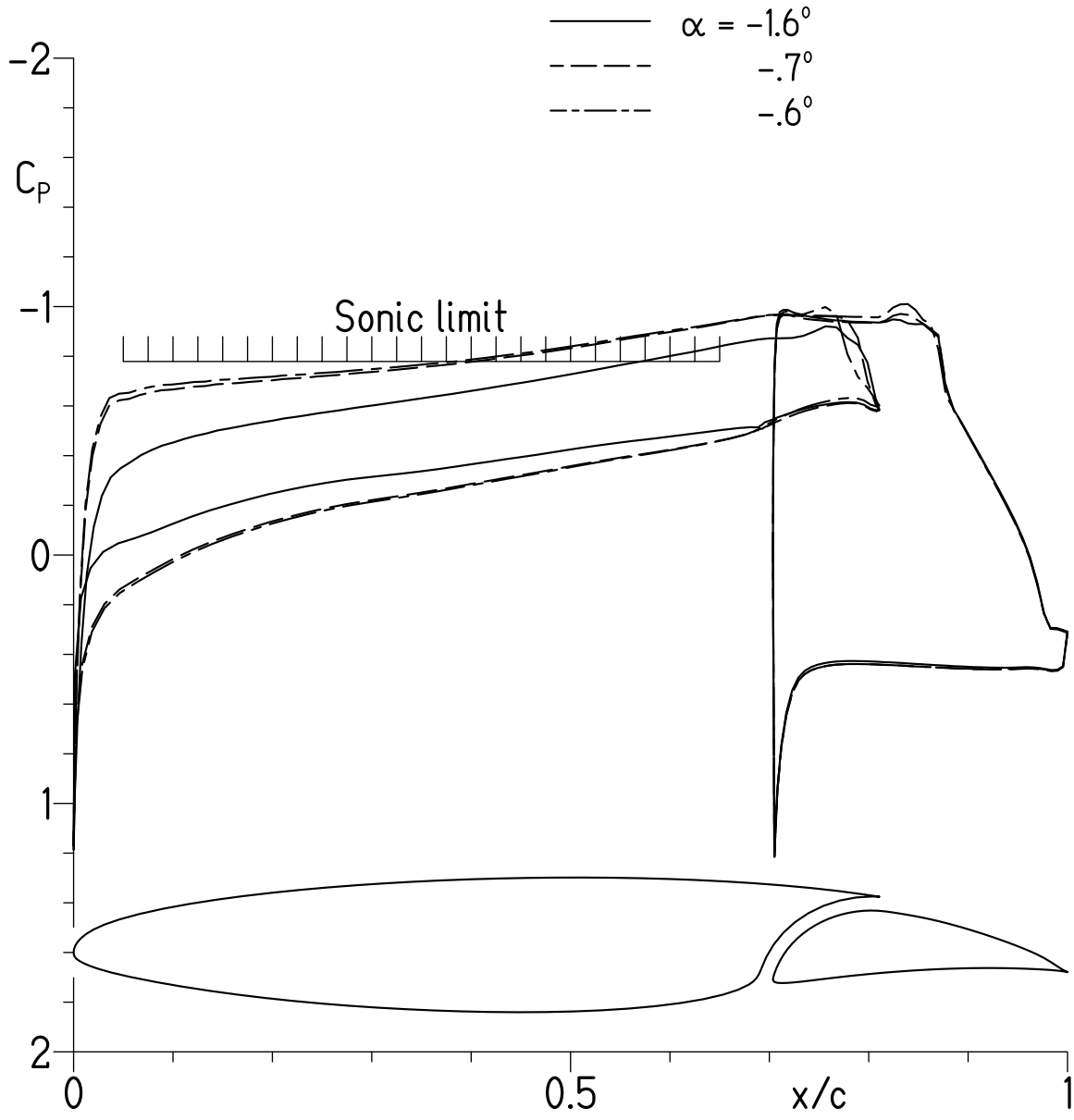

(b) $\alpha = -1.6°, -0.7°$, and $-0.6°$.

Figure 2.- Concluded.

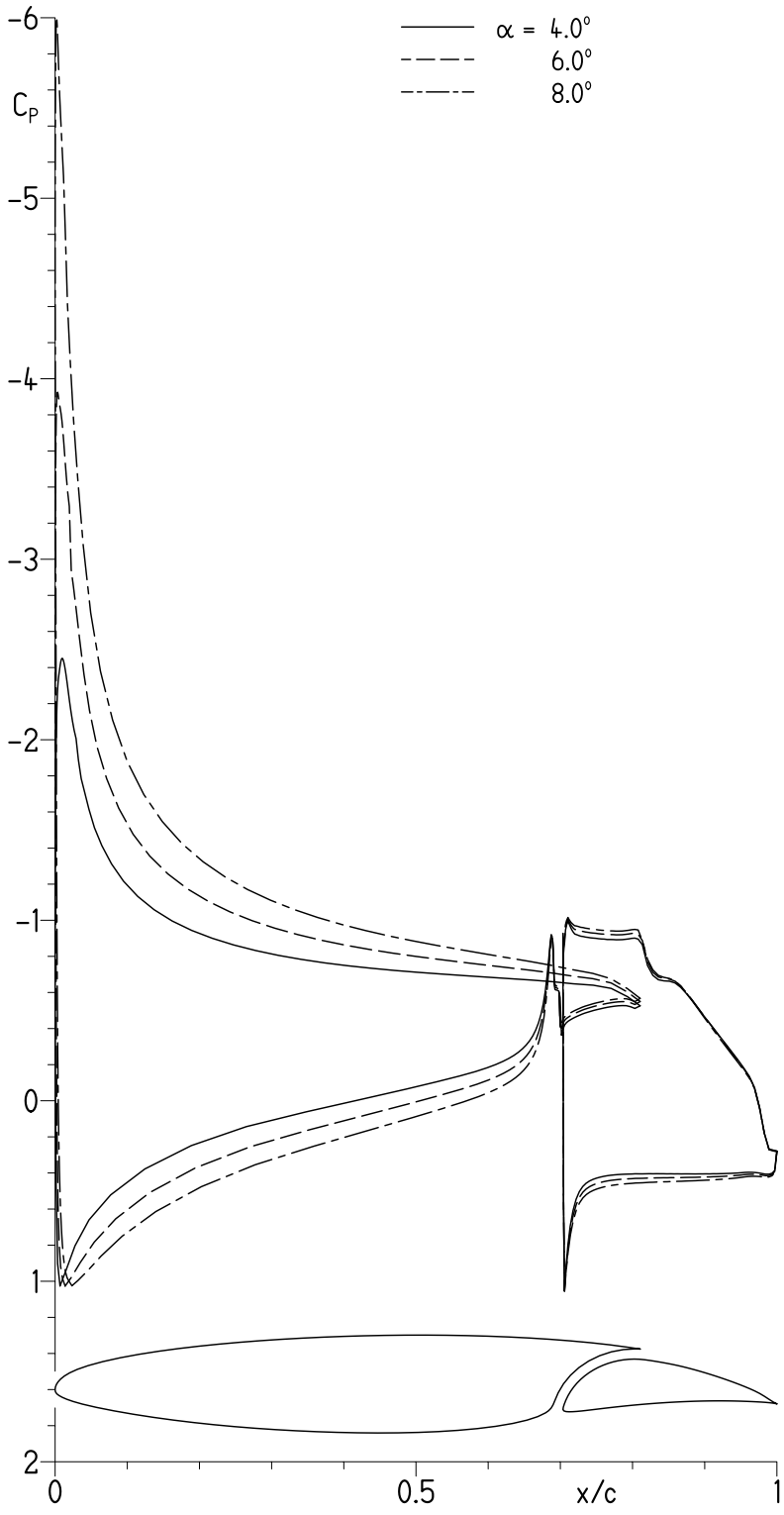

(a) $\alpha = 4.0°$, 6.0°, and 8.0°.

Figure 3.- Pressure distributions at $M = 0.225$ and $Re = 16.0 \times 10^6$ with transition free.

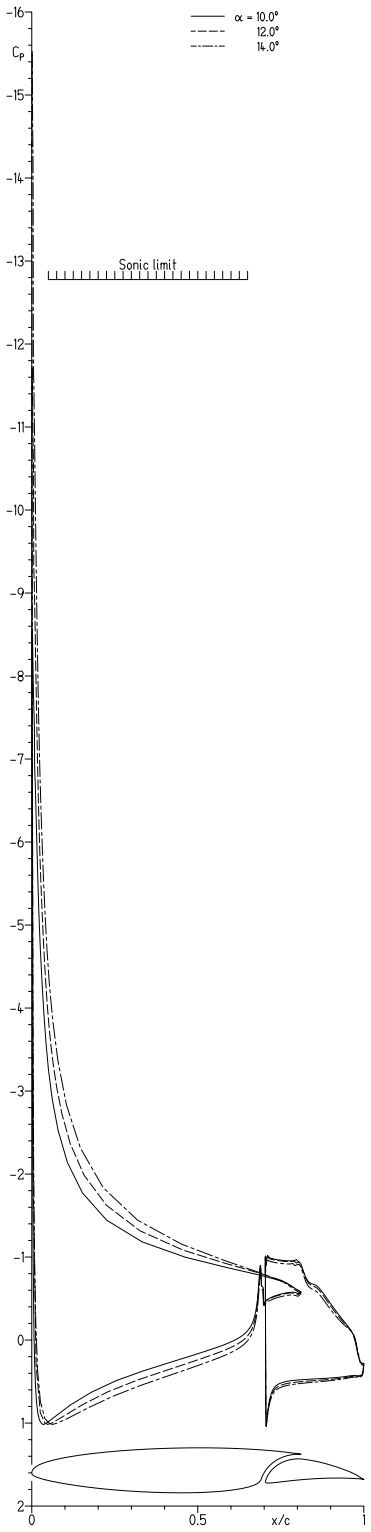

(b) $\alpha = 10.0°$, 12.0°, and 14.0°.

Figure 3.- Concluded.

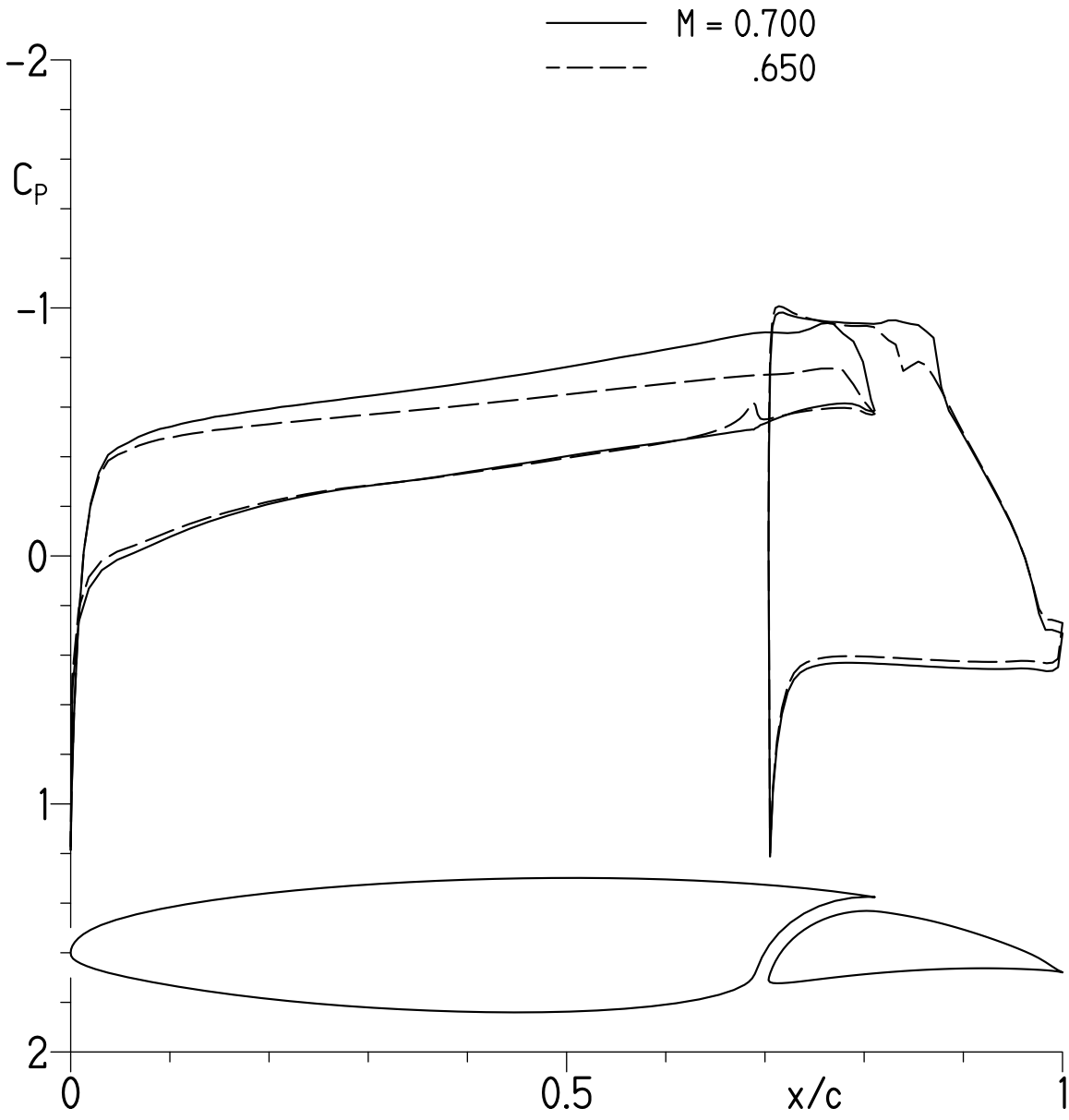

Figure 4.- Effect of Mach number on pressure distribution at $\alpha = -1.3°$ for $Re = 13.2 \times 10^6$ with transition free.

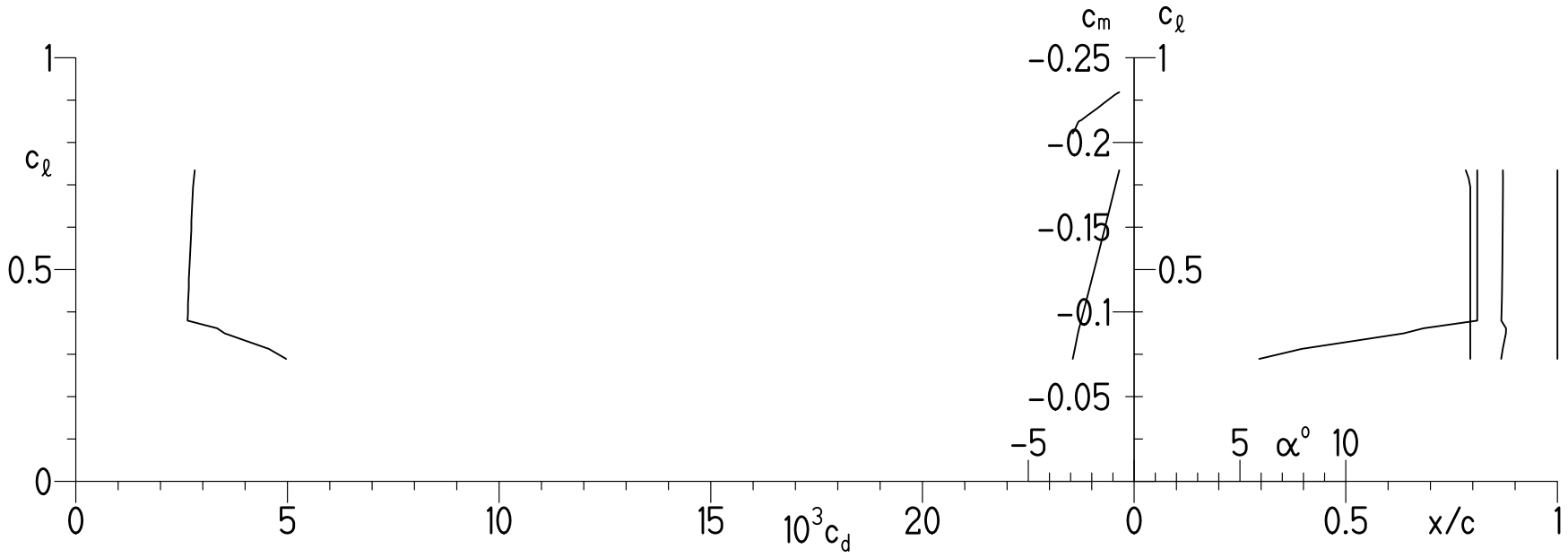

Figure 5.- Section characteristics at M = 0.700 and Re = 13.2×10^6 with transition free.

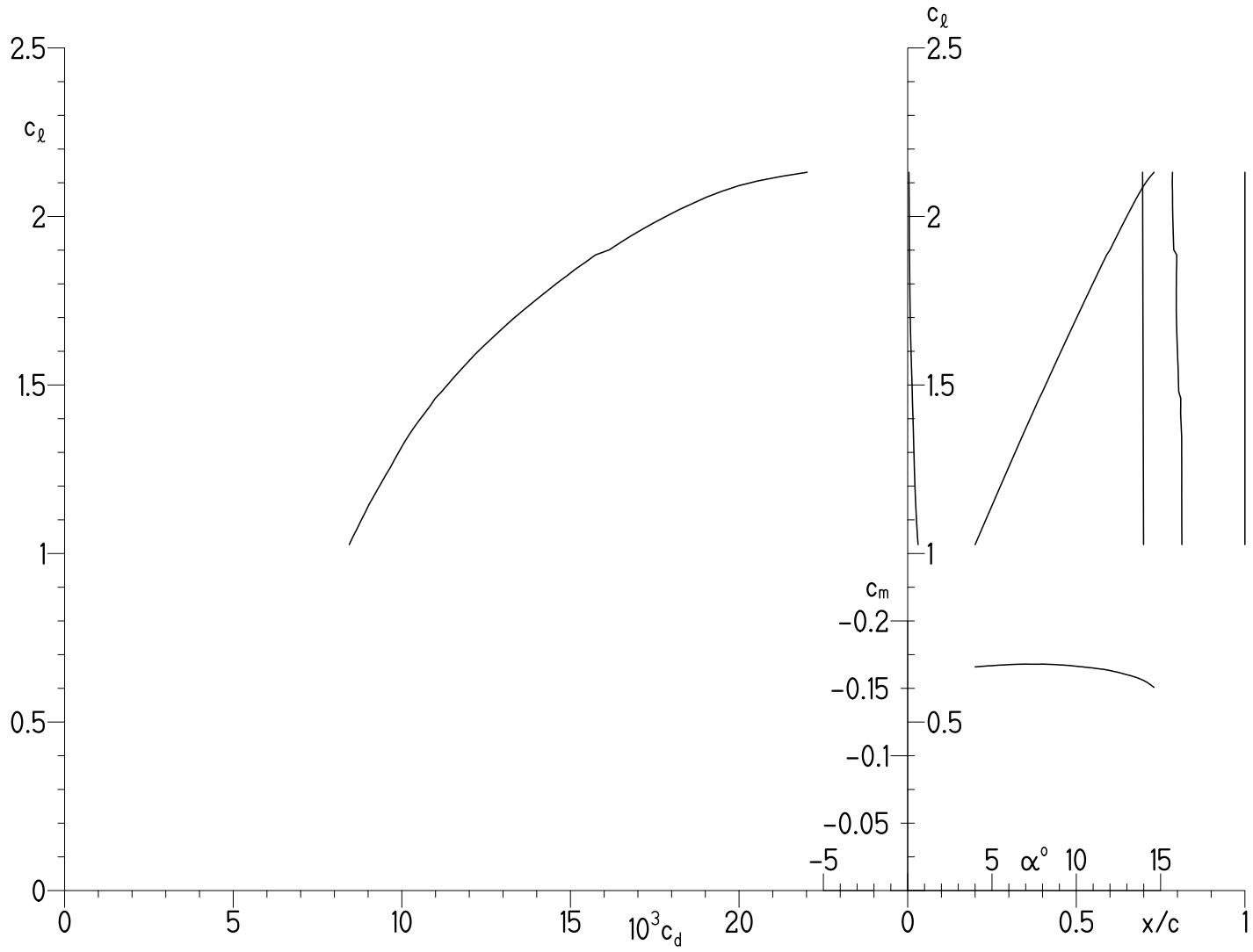

Figure 6.- Section characteristics at M = 0.225 and Re = 16.0×10^6 with transition free.

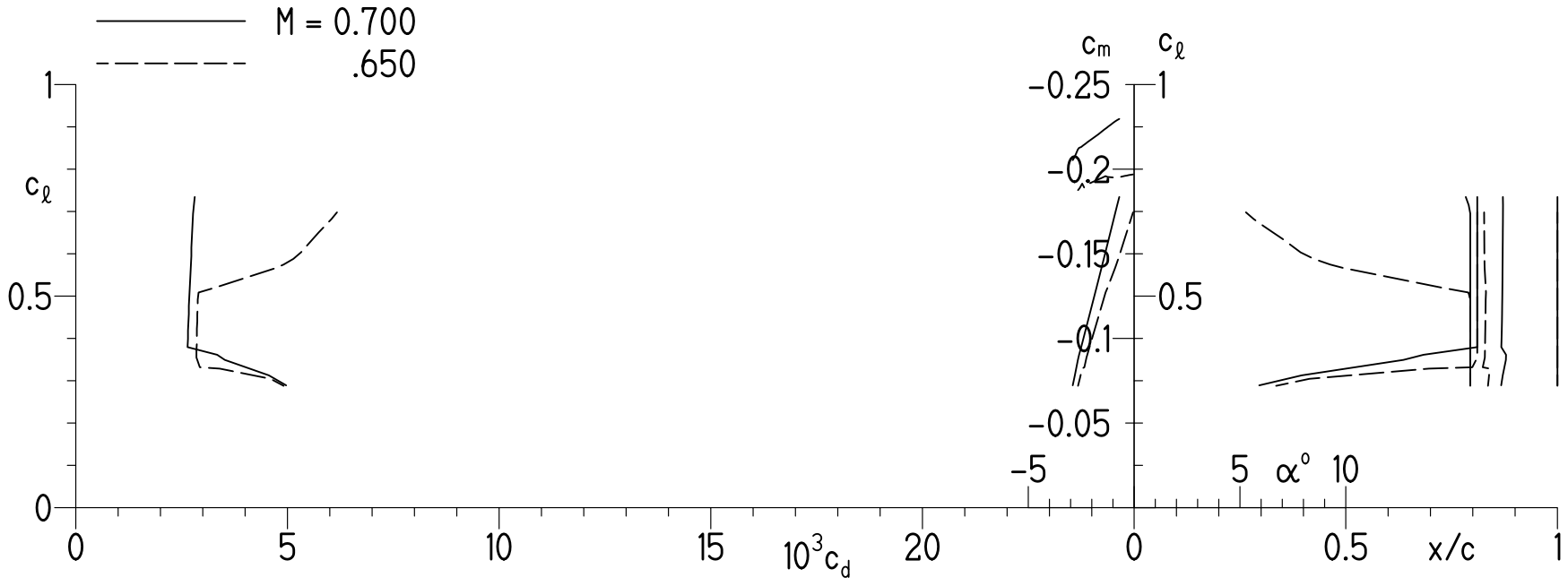

Figure 7.- Effect of Mach number on section characteristics for Re = 13.2×10^6 with transition free.

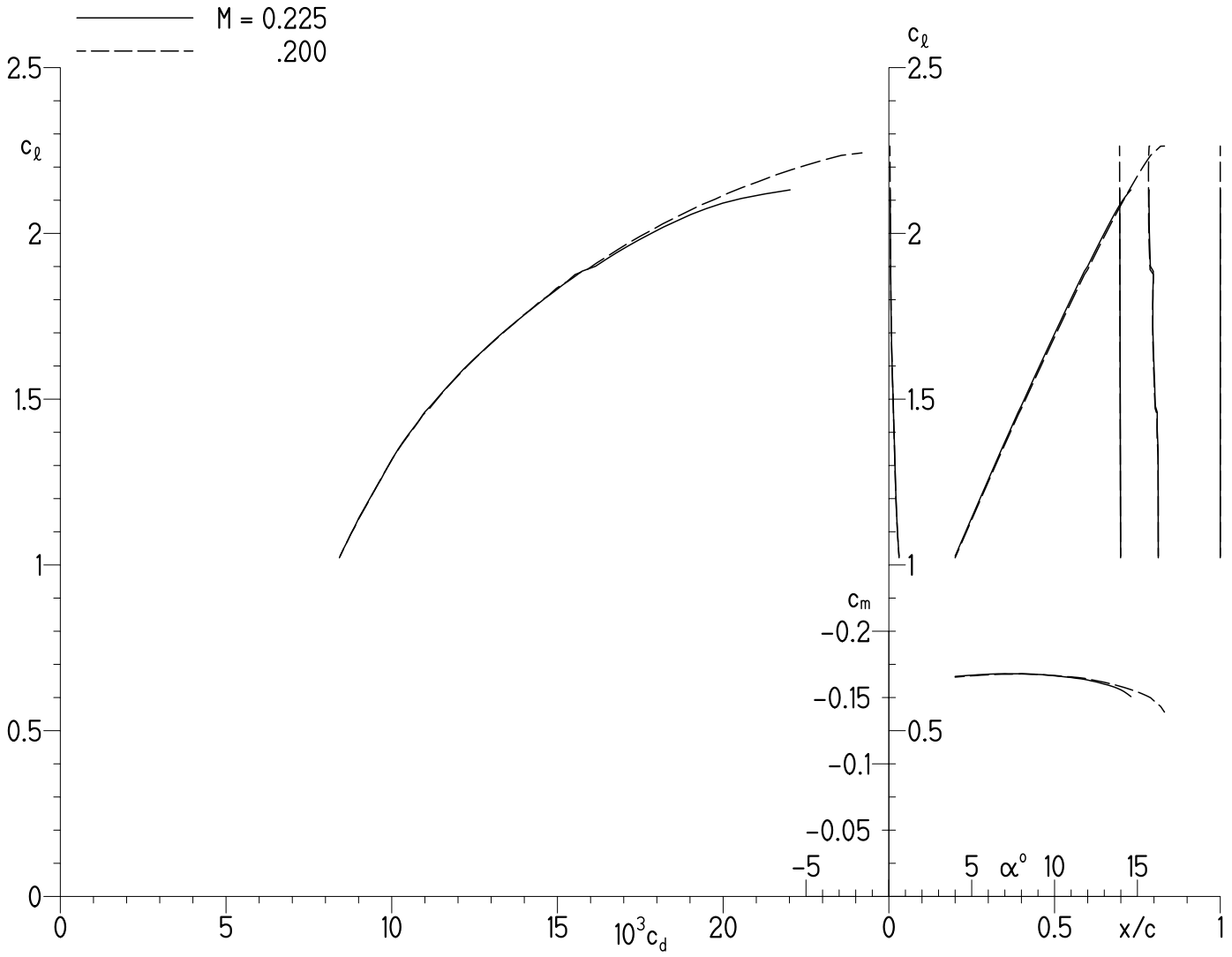

Figure 8.- Effect of Mach number on section characteristics for $Re = 16.0 \times 10^6$ with transition free.

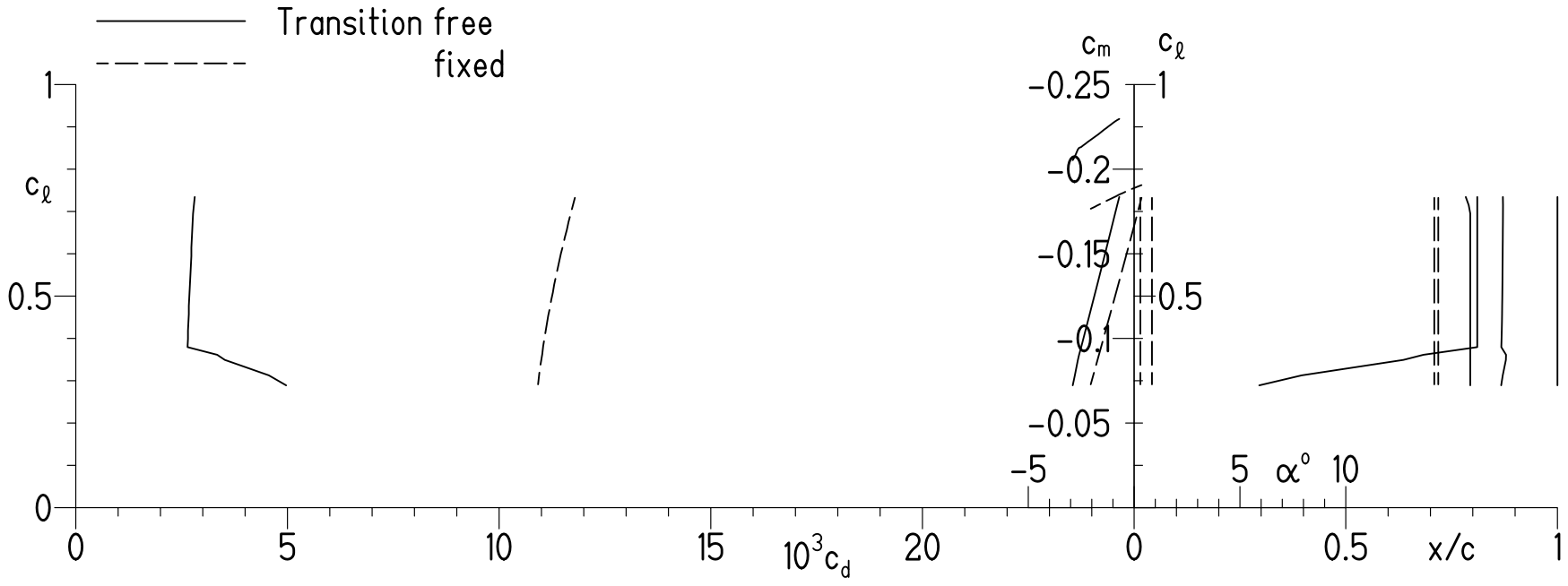

Figure 9.- Effect of fixing transition at M = 0.700 and Re = 13.2×10^6.

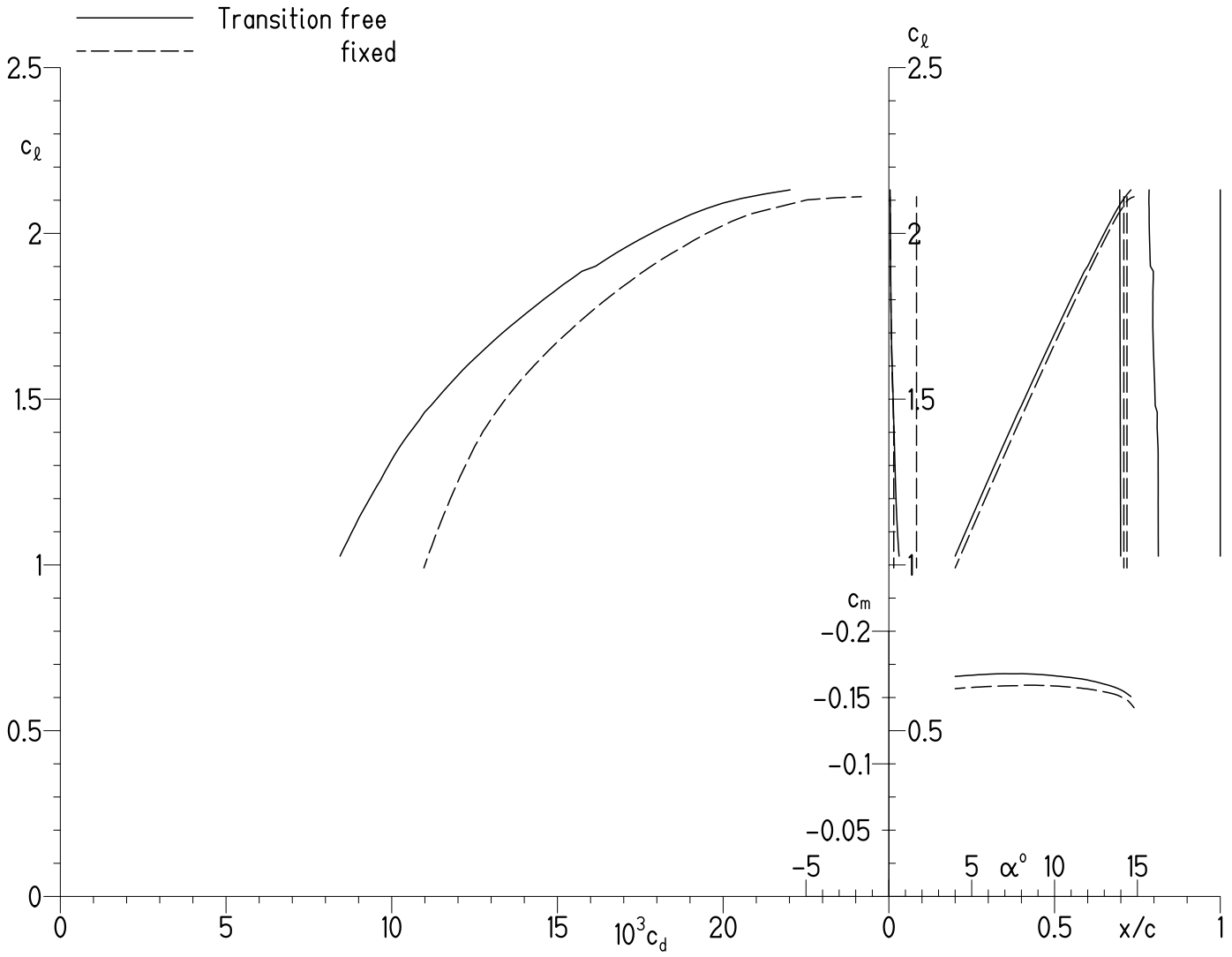

Figure 10.- Effect of fixing transition at M = 0.225 and Re = 16.0×10^6.

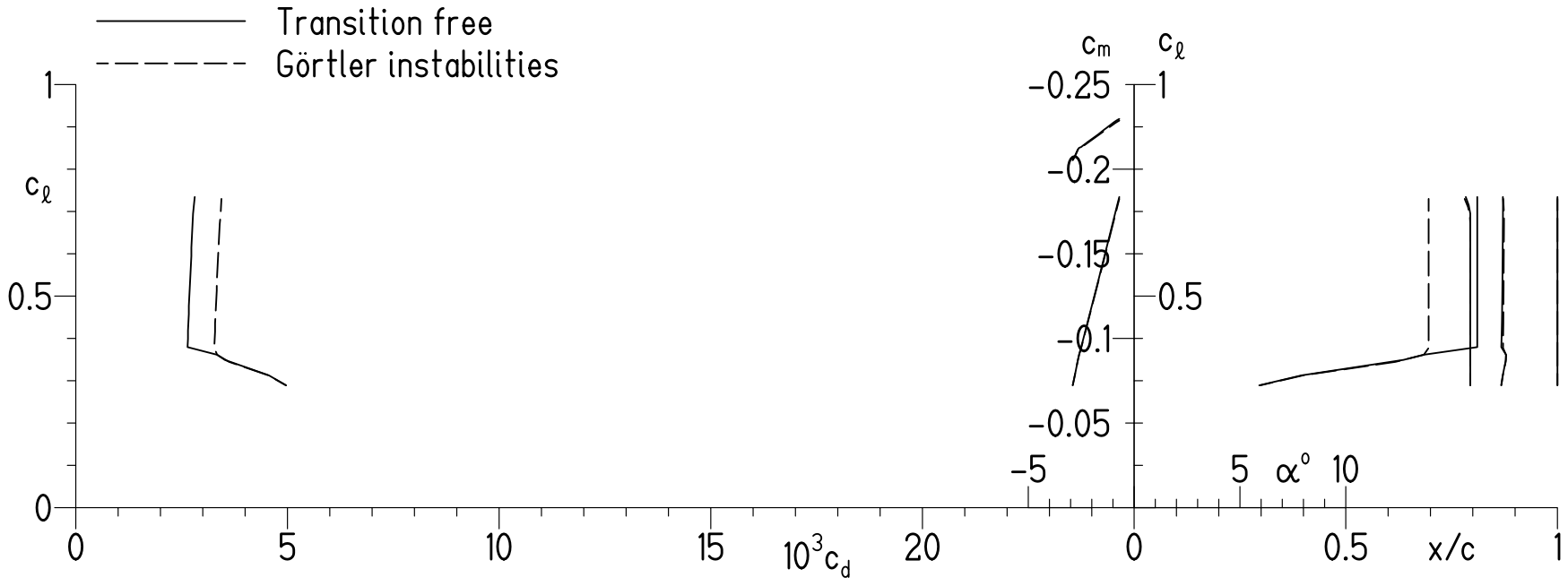

Figure 11.- Possible effect of Görtler instabilities on section characteristics at M = 0.700 and Re = 13.2×10^6.

REPORT DOCUMENTATION PAGE

Form Approved
OMB No. 0704-0188

1. REPORT DATE *(DD-MM-YYYY)*	2. REPORT TYPE	3. DATES COVERED *(From - To)*
01-09-2019	Contractor Report	

4. TITLE AND SUBTITLE

Design of a Slotted, Natural-Laminar-Flow Airfoil for a Transport Aircraft

5a. CONTRACT NUMBER
NNX17AJ95A

5b. GRANT NUMBER

5c. PROGRAM ELEMENT NUMBER

6. AUTHOR(S)
Somers, Dan M.

5d. PROJECT NUMBER

5e. TASK NUMBER

5f. WORK UNIT NUMBER
128698.02.93.07.45

7. PERFORMING ORGANIZATION NAME(S) AND ADDRESS(ES)
NASA Langley Research Center
Hampton, VA 23681-2199

8. PERFORMING ORGANIZATION REPORT NUMBER

9. SPONSORING/MONITORING AGENCY NAME(S) AND ADDRESS(ES)
National Aeronautics and Space Administration
Washington, DC 20546-0001

10. SPONSOR/MONITOR'S ACRONYM(S)
NASA

11. SPONSOR/MONITOR'S REPORT NUMBER(S)
NASA/CR-2019-220403

12. DISTRIBUTION/AVAILABILITY STATEMENT
Unclassified - Unlimited
Subject Category 02
Availability: NASA STI Program (757) 864-9658

13. SUPPLEMENTARY NOTES

Langley Technical Monitor: William E. Milholen

14. ABSTRACT

A 13.49-percent-thick, slotted, natural-laminar-flow airfoil, the S207, for a transport aircraft has been designed and analyzed theoretically. The two primary objectives of high maximum lift, insensitive to roughness, and low profile drag have been achieved. The dragdivergence Mach number is predicted to be greater than 0.70.

15. SUBJECT TERMS

natural laminar flow; slotted airfoil; transonic; transport aircraft

16. SECURITY CLASSIFICATION OF:			17. LIMITATION OF ABSTRACT	18. NUMBER OF PAGES	19a. NAME OF RESPONSIBLE PERSON
a. REPORT	b. ABSTRACT	c. THIS PAGE			STI Help Desk (email: help@sti.nasa.gov)
U	U	U	UU	33	19b. TELEPHONE NUMBER *(Include area code)* (757) 864-9658